

Contents lists available at ScienceDirect

# Physics Letters B

journal homepage: www.elsevier.com/locate/physletb



# Soft-gluon corrections for *tqZ* production

Nikolaos Kidonakis a,\*, Nodoka Yamanaka b,c

- <sup>a</sup> Department of Physics, Kennesaw State University, Kennesaw, GA 30144, USA
- b Kobayashi-Maskawa Institute for the Origin of Particles and the Universe, Nagoya University, Furocho, Chikusa, Aichi 464-8602, Japan
- <sup>c</sup> Nishina Center for Accelerator-Based Science, RIKEN, Wako 351-0198, Japan



Article history:
Received 18 October 2022
Received in revised form 28 December 2022
Accepted 17 January 2023
Available online 19 January 2023
Editor: A. Ringwald

### ABSTRACT

We study soft-gluon corrections for the associated production of a single top quark and a Z boson (tqZ production) at hadron colliders. We find that the radiative corrections are dominated by soft-gluon emission. We derive an approximate NNLO (aNNLO) cross section by adding second-order soft-gluon corrections to the exact NLO result. We calculate the aNNLO cross section at LHC energies, including uncertainties from scale dependence and from parton distributions. We also calculate differential distributions in top-quark rapidity. We show that the aNNLO corrections are significant and they enhance the NLO cross section while decreasing theoretical uncertainties.

© 2023 The Author(s). Published by Elsevier B.V. This is an open access article under the CC BY license (http://creativecommons.org/licenses/by/4.0/). Funded by SCOAP<sup>3</sup>.

# 1. Introduction

The production of a single top quark in association with a Z boson, i.e. tqZ production where q represents a light quark or antiquark, is an interesting process that is being studied at the LHC [1–6]. Searches for the process were already underway at 8 TeV LHC energy [1] with later measurements following at 13 TeV [2,3], and eventually leading to the observation of this process at 13 TeV collisions [4,5]. Further measurements, including differential cross sections, were made in [6].

The tqZ production processes allow for the t-Z and W-W-Z couplings to be studied in a single interaction. These processes can be affected by physics beyond the Standard Model, including flavor-changing neutral-current processes with anomalous top-quark couplings, such as t-q-Z [7–11] and t-q-g [12]. Top partner decays to tZ were considered in [13]. Furthermore, analyses for tqZ production in the context of SMEFT were presented in [14–16].

The tqZ processes also probe the anomalous "weak" moments of the top quark, whose interactions are defined as  $\mathcal{L}_{tZ} = C_t \bar{t} \sigma_{\mu\nu} (\partial^{\mu} Z^{\nu}) t + C_t' \bar{t} \sigma_{\mu\nu} (\partial^{\mu} Z^{\nu}) \gamma_5 t$ . These anomalous moments may be generated by new particles beyond the Standard Model appearing through loop diagrams in a similar way as the anomalous electromagnetic moments. On the other hand, these moments may also be probed by low-energy precision-test experiments. For instance, the top-quark weak dipole moment contributes to the electric dipole moments (EDMs) of light quarks through renormalization group evolution [17], and finally to the observable EDMs of the neutron and atoms [18]. However, the mixing between top-quark weak moments and the electromagnetic moments of light quarks occurs through the weak interaction, so a significant suppression happens. We then expect the direct production in accelerator experiments to have an important advantage over low-energy precision tests. We also note that the coupling between the top quark and the Z boson is larger than that between the top quark and the photon, so the sensitivity of tqZ production to new physics is potentially increased compared to  $tq\gamma$ , which is another advantage relative to the latter process.

Theoretical calculations for tqZ production are challenging since already at leading order (LO) the processes involve three particles in the final state, with two of them very massive, and four colored particles overall in the hard scattering. The next-to-leading-order (NLO) QCD corrections for tqZ production were calculated in [19]. The NLO electroweak (EW) corrections as well as off-shell effects were included in [20], with further work in [21]. The NLO QCD corrections turn out to be quite significant, providing an enhancement of around 16% to the LO cross section at LHC energies, while the NLO EW corrections are rather small, only 1%. Thus, it is important to consider further higher-order QCD corrections.

E-mail address: nkidonak@kennesaw.edu (N. Kidonakis).

<sup>\*</sup> Corresponding author.

Soft-gluon resummation [22–32] has long been known to be very important for top-quark processes, since the cross section receives large corrections from soft-gluon emission near partonic threshold due to the large mass of the top quark. This is well known for many  $2 \rightarrow 2$  top-quark processes, including top-antitop pair production [22,23,26,29], single-top production [25,27,28,30,31], and even processes beyond the Standard Model, for example involving top-quark anomalous couplings [7,9,10,12] (see e.g. the review in Ref. [33]). More recently, soft-gluon resummation has been applied to  $2 \rightarrow 3$  processes [32], in particular tqH production [34] and  $tq\gamma$  production [35]. In all these processes, as well as tqZ production, the soft-gluon corrections are dominant and account for the majority of the complete corrections at NLO. Furthermore, the soft-gluon calculations at next-to-next-to-leading order (NNLO) predicted very well the later complete NNLO results for top-antitop production and s-channel single-top production (see e.g. the review in Ref. [33]). These facts, along with the relevance of resummation in the related tZ production via anomalous couplings in [7,9,10], provide very strong motivation for the study of resummation for tqZ production.

In this paper, we use soft-gluon resummation to calculate approximate NNLO (aNNLO) cross sections for tqZ production, which are derived by adding second-order soft-gluon corrections to the exact NLO result. In the next section, we describe the resummation formalism and its specific implementation for tqZ production in single-particle-inclusive kinematics. In Section 3, we provide results for the total cross sections, including theoretical uncertainties, at LHC energies. In Section 4, we give results for the top-quark rapidity distributions. We conclude in Section 5.

### 2. Resummation for tqZ production

We begin with the soft-gluon resummation formalism for tqZ production, implementing the theoretical framework in [32]. We study the parton-level processes  $a(p_a)+b(p_b)\to t(p_t)+q(p_q)+Z(p_Z)$ , and we define the usual kinematical variables  $s=(p_a+p_b)^2$ ,  $t=(p_a-p_t)^2$ , and  $u=(p_b-p_t)^2$ . With an additional gluon emission in the final state, momentum conservation is given by  $p_a+p_b=p_t+p_q+p_Z+p_g$  where  $p_g$  is the gluon momentum. We then define a threshold variable  $s_4=(p_q+p_Z+p_g)^2-(p_q+p_Z)^2=s+t+u-m_t^2-(p_q+p_Z)^2$  which involves the extra energy from gluon emission and which vanishes as  $p_g\to 0$ .

We write the differential cross section for tqZ production in proton-proton collisions as a convolution,

$$d\sigma_{pp\to tqZ} = \sum_{a,b} \int dx_a \, dx_b \, \phi_{a/p}(x_a, \mu_F) \, \phi_{b/p}(x_b, \mu_F) \, d\hat{\sigma}_{ab\to tqZ}(s_4, \mu_F) \,, \tag{2.1}$$

where  $\mu_F$  is the factorization scale,  $\phi_{a/p}$  and  $\phi_{b/p}$  are parton distribution functions (pdf) for parton a and parton b, respectively, in the proton, and  $d\hat{\sigma}_{ab\to tqZ}$  is the partonic differential cross section.

The cross section factorizes if we take Laplace transforms [32], defined by

$$d\tilde{\hat{\sigma}}_{ab \to tqZ}(N, \mu_F) = \int_{0}^{s} \frac{ds_4}{s} e^{-Ns_4/s} d\hat{\sigma}_{ab \to tqZ}(s_4, \mu_F), \tag{2.2}$$

where N is the transform variable. Under transforms, the logarithms of  $s_4$  in the perturbative series go into logarithms of N which, as we will see, exponentiate. We also define transforms of the pdf via  $\tilde{\phi}(N) = \int_0^1 e^{-N(1-x)}\phi(x)\,dx$ . Replacing the colliding protons by partons in Eq. (2.1) [23,32,36], we thus have the factorized form in transform space

$$d\tilde{\sigma}_{ab\to taZ}(N) = \tilde{\phi}_{a/a}(N_a, \mu_F) \,\tilde{\phi}_{b/b}(N_b, \mu_F) \,d\tilde{\hat{\sigma}}_{ab\to taZ}(N, \mu_F) \,. \tag{2.3}$$

The cross section can be refactorized [22–24,32] in terms of an infrared-safe short-distance hard function,  $H_{ab\to tqZ}$ , and a soft function,  $S_{ab\to tqZ}$ , which describes the emission of noncollinear soft gluons. We have

$$d\tilde{\sigma}_{ab\to tqZ}(N) = \tilde{\psi}_{a/a}(N_a, \mu_F) \, \tilde{\psi}_{b/b}(N_b, \mu_F) \, \tilde{J}_q(N, \mu_F) \, \text{tr} \left\{ H_{ab\to tqZ} \left( \alpha_s(\mu_R) \right) \, \tilde{S}_{ab\to tqZ} \left( \frac{\sqrt{s}}{N\mu_F} \right) \right\}, \tag{2.4}$$

where  $\alpha_s$  is the strong coupling and  $\mu_R$  is the renormalization scale. The functions  $\psi$  are distributions for incoming partons at fixed value of momentum and involve collinear emission [22–24,36] while the function  $J_q$  describes radiation from the final-state light quark. The hard and the soft functions for the tqZ production processes are 2 × 2 matrices in the color space of the partonic scattering.

Comparing Eqs. (2.3) and (2.4), we find an expression for the hard-scattering partonic cross section in transform space

$$d\tilde{\hat{\sigma}}_{ab\to tqZ}(N,\mu_F) = \frac{\tilde{\psi}_{a/a}(N_a,\mu_F)\,\tilde{\psi}_{b/b}(N_b,\mu_F)\,\tilde{J}_q(N,\mu_F)}{\tilde{\phi}_{a/a}(N_a,\mu_F)\,\tilde{\phi}_{b/b}(N_b,\mu_F)}\,\operatorname{tr}\left\{H_{ab\to tqZ}\left(\alpha_s(\mu_R)\right)\,\tilde{S}_{ab\to tqZ}\left(\frac{\sqrt{s}}{N\mu_F}\right)\right\}. \tag{2.5}$$

The dependence of the soft matrix on the transform variable, N, is resummed via renormalization-group evolution [22,23]. Thus,  $\tilde{S}_{ab \to tqZ}$  obeys a renormalization-group equation in terms of a soft anomalous dimension matrix,  $\Gamma_{Sab \to tqZ}$ , which is calculated from the coefficients of the ultraviolet poles of the relevant eikonal diagrams [22–33].

The *N*-space resummed cross section, which resums logarithms of *N*, is derived from the renormalization-group evolution of the functions  $\tilde{S}_{ab\to tqZ}$ ,  $\tilde{\psi}$ ,  $\tilde{\phi}$ , and  $\tilde{J}_q$  in Eq. (2.5), and it is given by

$$d\tilde{\hat{\sigma}}_{ab\to tqZ}^{\text{resum}}(N,\mu_F) = \exp\left[\sum_{i=a,b} E_i(N_i)\right] \exp\left[\sum_{i=a,b} 2\int_{\mu_F}^{\sqrt{s}} \frac{d\mu}{\mu} \gamma_{i/i}(N_i)\right] \exp\left[E'_q(N)\right]$$

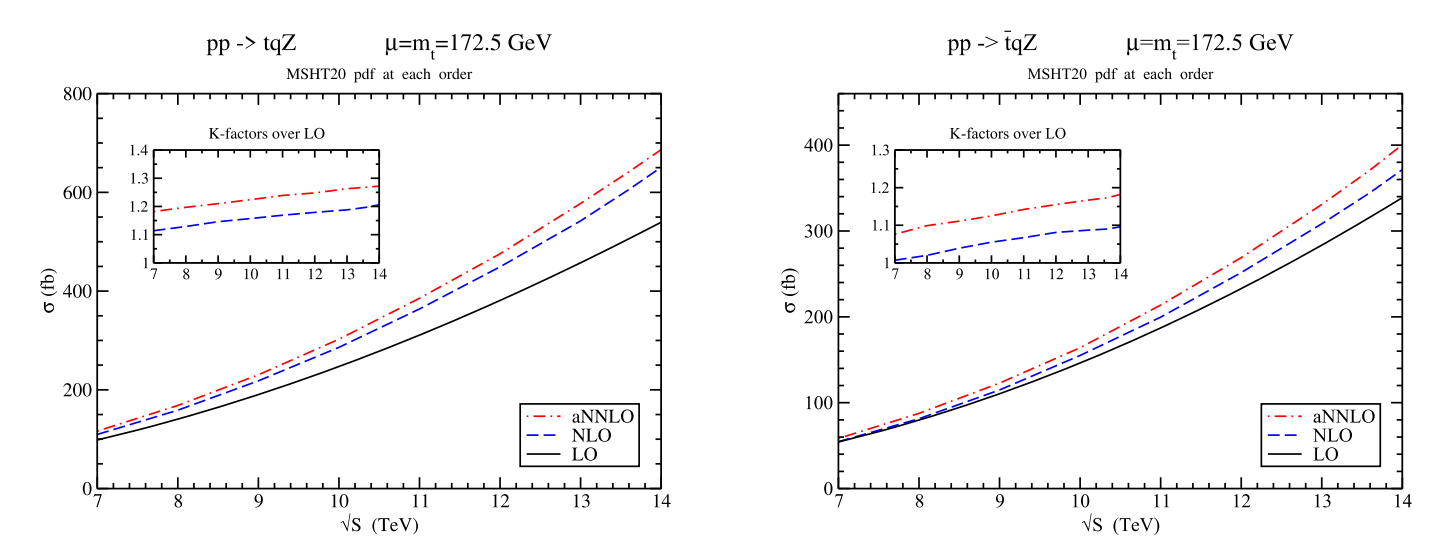


Fig. 1. The total cross sections for tqZ (left) and  $\bar{t}qZ$  (right) production in pp collisions at LHC energies.

$$\times \operatorname{tr} \left\{ H_{ab \to tqZ} \left( \alpha_{s}(\sqrt{s}) \right) \bar{P} \exp \left[ \int_{\sqrt{s}}^{\sqrt{s}/N} \frac{d\mu}{\mu} \Gamma_{Sab \to tqZ}^{\dagger} \left( \alpha_{s}(\mu) \right) \right] \right.$$

$$\times \tilde{S}_{ab \to tqZ} \left( \alpha_{s} \left( \frac{\sqrt{s}}{N} \right) \right) P \exp \left[ \int_{\sqrt{s}}^{\sqrt{s}/N} \frac{d\mu}{\mu} \Gamma_{Sab \to tqZ} \left( \alpha_{s}(\mu) \right) \right] \right\},$$

$$(2.6)$$

where P ( $\bar{P}$ ) denotes path-ordering in the same (reverse) sense as the integration variable  $\mu$ . The first exponential in Eq. (2.6) resums soft and collinear emission from the initial-state partons, and the second exponential involves the parton anomalous dimensions  $\gamma_{i/i}$  and the dependence on  $\mu_F$ , while the third exponential resums radiation from the final-state light quark (explicit expressions can be found in Ref. [32]). The last two exponentials involve integrals of the soft anomalous dimension matrix  $\Gamma_{S \, ab \to tqZ}$  and its Hermitian adjoint. The expressions for  $\Gamma_{S \, ab \to tqZ}$  at one and two loops can be found in Ref. [32] and they are simply related to similar expressions for single-top processes in [31]. The resummed cross section can be expanded at fixed order and then inverted to momentum space, without requiring a prescription, to produce numerical results. We note that we are not calculating virtual corrections at NNLO as the two-loop hard function is not known. Our aNNLO cross section is derived by matching the second-order expansion of the resummed soft-gluon cross section to the exact NLO result.

# 3. Total tqZ cross sections

In this section we present results for the total cross sections for tqZ production and, separately, for  $\bar{t}qZ$  production (i.e. with an antitop). We set the top-quark mass  $m_t = 172.5$  GeV, and the factorization and renormalization scales equal to each other, with this common scale denoted by  $\mu$ . The NLO results are found by using MadGraph5\_AMC@NLO [37]. We use MSHT20 [38] pdf in our calculations unless otherwise noted.

We first note that the soft-gluon corrections at NLO provide an excellent approximation to the exact NLO results. If we define the approximate NLO (aNLO) cross section as the sum of the LO cross section and the first-order soft-gluon corrections, then we find that the aNLO result is very close to the complete NLO one for LHC energies, with less than 1% difference, indicating that the overwhelming majority of the NLO corrections are accounted for in our formalism. We note that this is very similar to the findings for the related tZ production process via anomalous couplings [9,10]. This provides very strong motivation and justification for the calculation of aNNLO corrections.

Our aNNLO results are calculated by adding the second-order soft-gluon corrections to the exact NLO result; i.e., aNNLO=NLO+ soft aNNLO corrections. These aNNLO calculations provide our best theoretical prediction for the cross section.

In Fig. 1 we show results for the tqZ (left plot) and  $\bar{t}qZ$  (right plot) cross sections at LO, NLO, and aNNLO in pp collisions at LHC energies using MSHT20 pdf corresponding at each order. The inset plots show the K-factors relative to LO, i.e. the NLO/LO and the aNNLO/LO ratios. We see that the K-factors gradually increase as the energy goes from 7 to 14 TeV.

In Table 1 we show total rates for tqZ production for various LHC energies at LO, NLO, and aNNLO using MSHT20 pdf at each order. The central values are with a scale choice  $\mu=m_t=172.5$  GeV, the first uncertainty is from scale variation over the range  $m_t/2$  to  $2m_t$ , and the second uncertainty is from the MSHT20 pdf. The NLO corrections increase the LO cross section by 12% at 7 TeV, 13% at 8 TeV, 19% at 13 TeV, 20% at 13.6 TeV, and 21% at 14 TeV. The aNNLO corrections are also significant, providing a further increase of around 6% at 7 and 8 TeV, and around 7% at 13, 13.6, and 14 TeV. Furthermore, the scale dependence is reduced significantly at higher orders, and at aNNLO it becomes comparable to the pdf uncertainty. Thus, the aNNLO result provides a significantly improved theoretical prediction.

We note that the use of other recent pdf sets, i.e. CT18 pdf [39] and NNPDF4.0 pdf [40], gives NLO cross sections (with NLO pdf) that are almost identical to the ones we derived with MSHT20 pdf in both central value and scale uncertainty. For example, the NLO cross

**Table 1** The tqZ cross sections (in fb), with scale and pdf uncertainties, in pp collisions with  $\sqrt{S}=7$ , 8, 13, 13.6, and 14 TeV,  $m_t=172.5$  GeV, and MSHT20 pdf.

tqZ cross sections in pp collisions at the LHC								
$\sigma$ in fb	7 TeV	8 TeV	13 TeV	13.6 TeV	14 TeV			
LO NLO	$98.4_{-3.9-0.9}^{+1.6+1.6}$ $110 \pm 2_{-2}^{+1}$	$141^{+3}_{-7} \pm 2$ $159^{+3}_{-2} \pm 2$	$457^{+21+6}_{-32-3} \\ 542 \pm 11^{+6}_{-5}$	$506^{+24+6}_{-36-4} \\ 606^{+11}_{-12} \pm 6$	$540^{+26+6}_{-40-4} \\ 651^{+14}_{-16} \pm 6$			
aNNLO	$116^{+1}_{-2}\pm 2$	$168 \pm 2^{+3}_{-2}$	577_9_5	$641^{+4^{\circ}}_{-10^{\circ}-5}^{+6}$	$686^{+5}_{-13}^{+7}_{-5}$			

**Table 2** The  $\bar{t}qZ$  cross sections (in fb), with scale and pdf uncertainties, in pp collisions with  $\sqrt{S} = 7, 8, 13, 13.6$ , and 14 TeV,  $m_t = 172.5$  GeV, and MSHT20 pdf.

$\bar{t}qZ$ cross sections in $pp$ collisions at the LHC								
$\sigma$ in fb	7 TeV	8 TeV	13 TeV	13.6 TeV	14 TeV			
LO NLO aNNLO	$54.3^{+0.8}_{-2.1}^{+0.9}_{-1.2} \\ 54.6^{+1.3}_{-0.8}^{+1.3}_{-1.0} \\ 58.4^{+0.4}_{-0.7}^{+1.2}_{-1.0}$	79.7 <sup>+1.8</sup> +1.2 -3.6 <sup>-1.5</sup> 81.3 <sup>+1.9</sup> +1.7 87.6 <sup>+0.4</sup> +1.7 87.6 <sup>-1.2</sup> -1.4	$284^{+13+3}_{-20-5} \\ 308^{+8+5}_{-7-4} \\ 331^{+2}_{-6} \pm 4$	$316^{+15+3}_{-23-5}  345^{+8}_{-9} \pm 5  371^{+2}_{-8} \pm 4$	$\begin{array}{c} 339^{+17+3}_{-25-5} \\ 371^{+10+6}_{-9-4} \\ 401^{+2+5}_{-8-4} \end{array}$			

section at 13 TeV with CT18 pdf is  $541\pm11^{+14}_{-12}$  fb, and with NNPDF4.0 pdf it is  $538\pm11\pm3$  fb, while the corresponding result with MSHT20 pdf, as appears in Table 1, is  $542\pm11^{+6}_{-5}$  fb. At aNNLO (with NNLO pdf), the cross section with CT18 pdf is  $582^{+4+14}_{-9-13}$  fb, and with NNPDF4.0 pdf it is  $560^{+4}_{-9}\pm2$  fb, while the corresponding result with MSHT20 pdf, as given in Table 1, is  $577^{+4+6}_{-9-5}$  fb.

In Table 2 we show total rates for  $\bar{t}qZ$  production (i.e. with an antitop) for various LHC energies at LO, NLO, and aNNLO using MSHT20 pdf at each order. In this case, the NLO corrections are significantly smaller than for tqZ production while the aNNLO corrections are comparatively large, and one might worry about the convergence of the perturbative series. However, much of the difference between the aNNLO and NLO results in  $\bar{t}qZ$  production is due to the differences in the pdf used at each order. For example, at 13.6 TeV, using MSHT20 NNLO pdf for all orders, the  $\bar{t}qZ$  cross section is 320 fb at LO, 357 fb at NLO, and 371 fb at aNNLO. Also, the tqZ cross section at 13.6 TeV with MSHT20 NNLO pdf is 583 fb at LO, 627 fb at NLO, and 641 fb at aNNLO.

In addition to the scale and pdf uncertainties, one may want to give an estimate of uncertainty at aNNLO due to the approximation. There is no standard way of doing that, but one possibility would be to consider the relative difference between the aNLO and the full NLO corrections, and apply this uncertainty to the aNNLO corrections. Doing so, we find an additional uncertainty which is smaller than the scale and the pdf uncertainties. For example, for the tqZ cross section at 13 TeV, we find a 2 fb additional uncertainty at aNNLO which, as can be seen from Table 1, is smaller than the scale and pdf ones and which, even when added to the aNNLO scale and pdf uncertainties, gives an overall uncertainty at aNNLO that is smaller than that at NLO.

Finally, we note that the experimental data from the LHC use a variety of selection cuts, for example on the transverse momentum of the *Z*-boson or the light-quark jet, in the process. Our calculation is inclusive with respect to colored particles, and it is beyond the scope of this paper to do a detailed analysis with cuts on jets which, in any case, vary by experiment. However, we have investigated the dependence of the *K*-factors and also the fractional scale and pdf uncertainties of the cross section on some typical choices for cuts on the *Z* boson in this process at the 13 TeV LHC, and we find negligible dependence. For example, with a restriction that the transverse momentum of the *Z* boson be greater than 30 GeV, the *K*-factors remain virtually identical (less than one per mille difference) with those of the full cross section without cuts. The fractional scale and pdf uncertainties also remain virtually identical.

# 4. Top-quark rapidity distributions

Next, we present the top-quark rapidity  $(y_t)$  distributions in tqZ production, which provide more information than total cross sections. We present results at 13, 13.6, and 14 TeV energies.

Fig. 2 shows the top-quark rapidity distributions in tqZ production at 13 TeV LHC energy. The LO, NLO, and aNNLO results are plotted for the distribution of the absolute value of the top-quark rapidity,  $d\sigma/d|y_t|$ . The K-factors are shown in the inset plot. The aNNLO/LO line clearly increases at very high values of the top-quark rapidity. As we discussed for the total cross sections, part of the difference between the aNNLO and NLO results is due to the different pdf, especially at large rapidities.

Fig. 3 shows the LO, NLO, and aNNLO top-quark rapidity distributions in tqZ production at 13.6 TeV LHC energy, with the K-factors in the inset plot. Again, we observe significant enhancements from the aNNLO crorrections, especially at large rapidities.

Fig. 4 shows the LO, NLO, and aNNLO top-quark rapidity distributions in tqZ production at 14 TeV LHC energy. The K-factors in the inset plot show, again, the importance of the aNNLO corrections, particularly at large  $y_t$ .

Finally, we discuss the scale and pdf uncertainties in the rapidity distributions. For central and moderate values of the rapidity, up to a rapidity value of 2, the fractional scale and pdf uncertainties of the rapidity distribution at each order are essentially the same as those for the corresponding total cross section. However, for large rapidity values both the scale and the pdf uncertainties get bigger. At a rapidity value of 2.5, the fractional scale uncertainty is double that of the total cross section, while at a rapidity value of 3 it is triple. Also, the fractional pdf uncertainty is three times bigger than that of the total cross section at a rapidity value of 2.5 and six times bigger at a rapidity value of 3.

## 5. Conclusions

We have calculated higher-order QCD corrections, and more specifically soft-gluon corrections, for the associated production of a single top quark with a Z boson, which is a process that has been actively studied at the LHC. The NLO QCD corrections are very significant and,

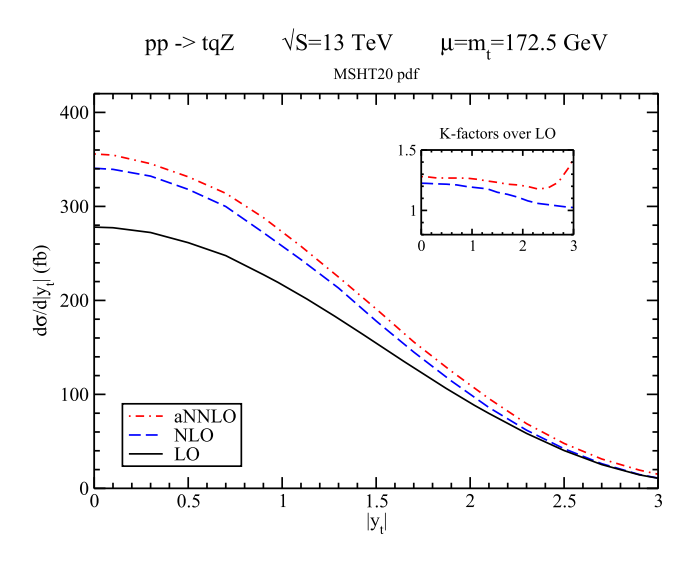


Fig. 2. The top-quark rapidity distributions in tqZ production at 13 TeV LHC energy.

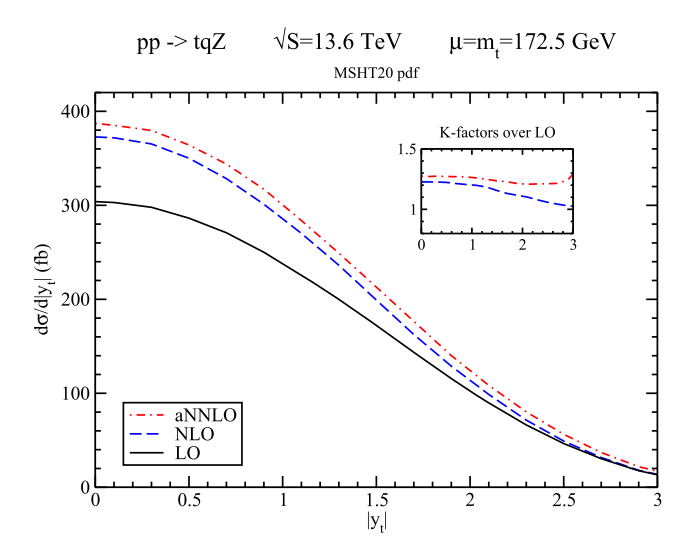


Fig. 3. The top-quark rapidity distributions in tqZ production at 13.6 TeV LHC energy.

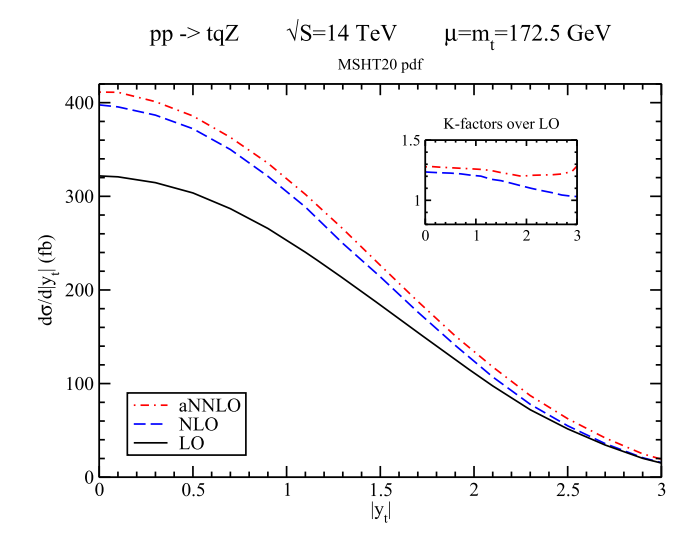


Fig. 4. The top-quark rapidity distributions in tqZ production at 14 TeV LHC energy.

thus, it is important to consider even higher-order corrections. By comparing the soft-gluon corrections at NLO with the complete NLO result, we have found that the corrections are dominated by soft-gluon emission. Thus, the calculation of aNNLO cross sections, i.e. the complete NLO result plus second-order soft-gluon corrections, is an important step towards producing better theoretical predictions.

We have found that the aNNLO corrections, which are derived from soft-gluon resummation, are very significant and increase the NLO cross section at LHC energies. We have also calculated theoretical uncertainties from scale variation and from pdf. We have found that the scale uncertainties decrease with each higher perturbative order. The pdf uncertainties remain relatively small at all orders.

Finally, we have calculated the rapidity distributions of the top quark at LO, NLO, and aNNLO. There are significant enhancements from the aNNLO corrections, particularly at larger rapidity values.

Our results provide the highest-order and up-to-date theoretical predictions for tqZ production at past, current, and future LHC energies. The improved precision is important as this process is sensitive to various couplings of the top quark and the W and Z bosons, and it can probe anomalous weak moments of the top quark.

# **Declaration of competing interest**

The authors declare that they have no known competing financial interests or personal relationships that could have appeared to influence the work reported in this paper.

### Data availability

No data was used for the research described in the article.

## Acknowledgements

We thank Matthew Forslund for early contributions to this work. The work of N.K. is supported by the National Science Foundation under Grant No. PHY 2112025. N.Y. was supported by Daiko Foundation.

#### References

- [1] CMS Collaboration, Search for associated production of a Z boson with a single top quark and for tZ flavour-changing interactions in pp collisions at  $\sqrt{s} = 8$  TeV, J. High Energy Phys. 07 (2017) 003, arXiv:1702.01404.
- [2] ATLAS Collaboration, Measurement of the production cross-section of a single top quark in association with a Z boson in proton-proton collisions at 13 TeV with the ATLAS detector, Phys. Lett. B 780 (2018) 557, arXiv:1710.03659.
- [3] CMS Collaboration, Measurement of the associated production of a single top quark and a Z boson in pp collisions at  $\sqrt{s} = 13$  TeV, Phys. Lett. B 779 (2018) 358, arXiv:1712.02825.
- [4] CMS Collaboration, Observation of single top quark production in association with a Z boson in proton-proton collisions at  $\sqrt{s} = 13$  TeV, Phys. Rev. Lett. 122 (2019) 132003. arXiv:1812.05900.
- [5] ATLAS Collaboration, Observation of the associated production of a top quark and a Z boson in pp collisions at  $\sqrt{s} = 13$  TeV with the ATLAS detector, J. High Energy Phys. 07 (2020) 124, arXiv:2002.07546.
- [6] CMS Collaboration, Inclusive and differential cross section measurements of single top quark production in association with a Z boson in proton-proton collisions at  $\sqrt{s} = 13$  TeV, J. High Energy Phys. 02 (2022) 107, arXiv:2111.02860.
- [7] N. Kidonakis, A. Belyaev, FCNC top quark production via anomalous tqV couplings beyond leading order, J. High Energy Phys. 12 (2003) 004, arXiv:hep-ph/0310299.
- [8] B.H. Li, Y. Zhang, C.S. Li, J. Gao, H.X. Zhu, Next-to-leading order QCD corrections to tZ associated production via the flavor-changing neutral-current couplings at hadron colliders, Phys. Rev. D 83 (2011) 114049, arXiv:1103.5122.
- [9] N. Kidonakis, Higher-order corrections for tZ production via anomalous couplings, Phys. Rev. D 97 (2018) 034028, arXiv:1712.01144.
- [10] M. Guzzi, N. Kidonakis, tZ' production at hadron colliders, Eur. Phys. J. C 80 (2020) 467, arXiv:1904.10071.
- [11] Y.-B. Liu, S. Moretti, Probing tqZ anomalous couplings in the trilepton signal at the HL-LHC, HE-LHC and FCC-hh, Chin. Phys. C 45 (2021) 043110, arXiv:2010.05148.
- [12] N. Kidonakis, E. Martin, Soft-gluon corrections in FCNC top-quark production via anomalous gluon couplings, Phys. Rev. D 90 (2014) 054021, arXiv:1404.7488.
- [13] J. Reuter, M. Tonini, Top partner discovery in the  $T \rightarrow tZ$  channel at the LHC, J. High Energy Phys. 01 (2015) 088, arXiv:1409.6962.
- [14] C. Degrande, F. Maltoni, K. Mimasu, E. Vryonidou, C. Zhang, Single-top associated production with a Z or H boson at the LHC: the SMEFT interpretation, J. High Energy Phys. 10 (2018) 005, arXiv:1804.07773.
- [15] R.K. Barman, A. Ismail, Constraining the top electroweak sector of the SMEFT through Z associated top pair and single top production at the HL-LHC, arXiv:2205.07912.
- [16] R. Mammen Abraham, D. Goncalves, Boosting new physics searches in  $t\bar{t}Z$  and tZj production with angular moments, arXiv:2208.05986.
- [17] V. Cirigliano, W. Dekens, J. de Vries, E. Mereghetti, Is there room for CP violation in the top-Higgs sector?, Phys. Rev. D 94 (2016) 016002, arXiv:1603.03049.
- [18] N. Yamanaka, B.K. Sahoo, N. Yoshinaga, T. Sato, K. Asahi, B.P. Das, Probing exotic phenomena at the interface of nuclear and particle physics with the electric dipole moments of diamagnetic atoms: a unique window to hadronic and semi-leptonic CP violation, Eur. Phys. J. A 53 (2017) 54, arXiv:1703.01570.
- [19] J. Campbell, R.K. Ellis, R. Rontsch, Single top production in association with a Z boson at the LHC, Phys. Rev. D 87 (2013) 114006, arXiv:1302.3856.
- [20] D. Pagani, I. Tsinikos, E. Vryonidou, NLO QCD+EW predictions for tHj and tZj production at the LHC, J. High Energy Phys. 08 (2020) 082, arXiv:2006.10086.
- [21] A. Denner, G. Pelliccioli, C. Schwan, NLO QCD and EW corrections to off-shell tZj production at the LHC, J. High Energy Phys. 10 (2022) 125, arXiv:2207.11264.
- [22] N. Kidonakis, G. Sterman, Subleading logarithms in QCD hard scattering, Phys. Lett. B 387 (1996) 867.
- [23] N. Kidonakis, G. Sterman, Resummation for QCD hard scattering, Nucl. Phys. B 505 (1997) 321, arXiv:hep-ph/9705234.
- [24] N. Kidonakis, G. Oderda, G. Sterman, Evolution of color exchange in QCD hard scattering, Nucl. Phys. B 531 (1998) 365, arXiv:hep-ph/9803241.
- [25] N. Kidonakis, Single top production at the Tevatron: threshold resummation and finite-order soft gluon corrections, Phys. Rev. D 74 (2006) 114012, arXiv:hep-ph/0609287.
- [26] N. Kidonakis, Two-loop soft anomalous dimensions and NNLL resummation for heavy quark production, Phys. Rev. Lett. 102 (2009) 232003, arXiv:0903.2561.
- [27] N. Kidonakis, NNLL resummation for s-channel single top quark production, Phys. Rev. D 81 (2010) 054028, arXiv:1001.5034.
- [28] N. Kidonakis, Two-loop soft anomalous dimensions for single top quark associated production with a W<sup>-</sup> or H<sup>-</sup>, Phys. Rev. D 82 (2010) 054018, arXiv:1005.4451.
- [29] N. Kidonakis, Next-to-next-to-leading soft-gluon corrections for the top quark cross section and transverse momentum distribution, Phys. Rev. D 82 (2010) 114030, arXiv:1009.4935.
- [30] N. Kidonakis, Next-to-next-to-leading-order collinear and soft gluon corrections for t-channel single top quark production, Phys. Rev. D 83 (2011) 091503, arXiv:1103. 2792.
- [31] N. Kidonakis, Soft anomalous dimensions for single-top production at three loops, Phys. Rev. D 99 (2019) 074024, arXiv:1901.09928.
- [32] M. Forslund, N. Kidonakis, Resummation for  $2 \rightarrow n$  processes in single-particle-inclusive kinematics, Phys. Rev. D 102 (2020) 034006, arXiv:2003.09021.
- [33] N. Kidonakis, Soft-gluon corrections in top-quark production, Int. J. Mod. Phys. A 33 (2018) 1830021, arXiv:1806.03336.
- [34] M. Forslund, N. Kidonakis, Soft-gluon corrections for the associated production of a single top quark and a Higgs boson, Phys. Rev. D 104 (2021) 034024, arXiv: 2103.01228.

- [35] N. Kidonakis, N. Yamanaka, QCD corrections in  $tq\gamma$  production at hadron colliders, Eur. Phys. J. C 82 (2022) 670, arXiv:2201.12877. [36] G. Sterman, Summation of large corrections to short-distance hadronic cross sections, Nucl. Phys. B 281 (1987) 310.
- [37] J. Alwall, et al., The automated computation of tree-level and next-to-leading order differential cross sections, and their matching to parton shower simulations, J. High Energy Phys. 07 (2014) 079, arXiv:1405.0301.
- [38] S. Bailey, T. Cridge, L.A. Harland-Lang, A.D. Martin, R.S. Thorne, Parton distributions from LHC, HERA, Tevatron and fixed target data: MSHT20 PDFs, Eur. Phys. J. C 81 (2021) 341, arXiv:2012.04684.
- [39] T.-J. Hou, et al., New CTEQ global analysis of quantum chromodynamics with high-precision data from the LHC, Phys. Rev. D 103 (2021) 014013, arXiv:1912.10053.
- [40] R.D. Ball, et al., The path to proton structure at one-percent accuracy, Eur. Phys. J. C 82 (2022) 428, arXiv:2109.02653.